

Dynamics of argon in confined geometry

K. Schmalzl¹, D. Wallacher², M.M. Koza³, M. Rheinstädter³, D. Strauch⁴
and K. Knorr²

¹ Forschungszentrum Jülich, 52425 Jülich, Germany

² Universität des Saarlandes, 66041 Saarbrücken, Germany

³ Institut Laue-Langevin, 38042 Grenoble, France

⁴ Universität Regensburg, 93040 Regensburg, Germany

Abstract. The role of geometrical confinement on the dynamics of argon is studied. We have investigated ³⁶Argon adsorbed in nanoporous Gelsil glass by inelastic neutron scattering. By fractional filling the ‘dimensionality’ of the system is tuned from a two-dimensional towards the bulk state. Ab-initio calculations of plane sheets of Ar atoms and of bulk Ar are compared to the experimental results. A shift of various phonon modes to lower energies with decreasing dimensionality is observed in the results of both methods.

1 Introduction

It is well established that geometrical confinement modifies the properties of a material [1]. This can be a free surface, an interface, an adsorbate layer, a free-standing film, etc. (in two dimensions) or quantum wires, thin tubes, etc. (in one dimension). In this study we have investigated by inelastic neutron scattering experiments the dynamics of ³⁶Ar adsorbed in nanoporous Gelsil glass. Primarily we focus here on a three layer and a bulk adsorbate. Additionally, we confront phonon dynamics calculations of a three layer and a bulk Ar system with experimental findings.

2 Theory

2.1 Bulk Argon

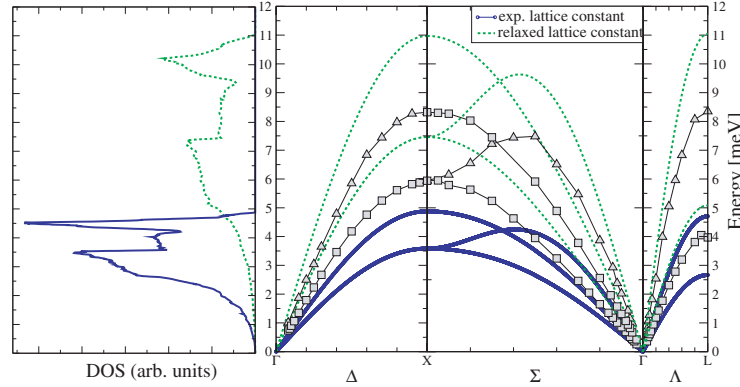
The calculations have been performed using density functional and density functional perturbation theory as implemented in the ABINIT code employing a plane-wave basis set and pseudopotentials [2]. As is well known, noble-gas crystals are difficult to describe within the conventional approximations. For this reason, we have checked two pseudopotentials, Hartwigsen-Goedecker-Hutter (HGH) and Troullier-Martins (TM), and the LDA and GGA (Perdew-Burke-Ernzerhof functional (PBE)) versions of the exchange-correlation potentials.

Table 1 shows the calculated and experimentally obtained lattice constants of fcc Ar. In the calculation a $4 \times 4 \times 4$ k-point mesh was used. As in many other cases, the lattice constant is underestimated in LDA and overestimated in GGA. The relaxed lattice constant gives better agreement within LDA than GGA, where the deviation by more than 11% is rather high.

The calculated phonon dispersion in the three main-symmetry directions and the corresponding DOS of bulk Ar for the relaxed and experimental lattice constant is shown in Fig. 1. The results have been calculated with TM pseudopotentials for the two lattice constants in LDA and with a cut-off $E_{\text{cut}} = 40$ Ha and are compared with experimental data from neutron scattering [3]. The calculations were done also with the HGH pseudopotential (not shown

Table 1. Comparison of the calculated lattice constant a (in Å) with the experimental value.

| Pseudopotential | E_{cut} [Ha] (Hartree) | a [Å] | dev. from exp. |
|-----------------|---------------------------------|---------|----------------|
| HGH (LDA) | 53 | 4.938 | -7% |
| TM (LDA) | 40 | 4.989 | -6.1% |
| TM (GGA-PBE) | 55 | 5.944 | 11.9% |
| Exp. (10K)[3] | | 5.31 | |

**Fig. 1.** Right: calculated phonon dispersion for the relaxed and experimental lattice constant in the three main-symmetry directions in comparison with experimental data from neutron scattering [3]. Squares refer to modes of transverse polarisation, triangles to modes of longitudinal polarisation. Lines are guide to the eye. Left: corresponding density of states (DOS).

here); the resulting frequencies are only slightly different from those using the TM pseudopotential. For the experimental lattice constant, the frequencies are about 1.8 times smaller than the experimental results, for a_{relax} the experimental data are overestimated by a factor of about 1.3. As expected, a comparison between frequencies computed with TM for a_{relax} and for a_{exp} shows a decrease of frequencies with increasing lattice constant in agreement with Ref. [4]. However, both calculated DOS show identical features providing confidence in the predictability of the dynamics of argon systems.

2.2 Argon layers

Starting from the hexagonal description of fcc bulk Ar resulting in $a_{\text{hex}} = 3.527 \text{ \AA}$ and $c_{\text{hex}} = 8.639 \text{ \AA}$ we constructed a system of three hexagonal layers with periodicity in the a - and b -direction and ABC-stacking with “vacuum” along c , see the sketch on the left panel of Fig. 2. After relaxation of a_{hex} and c_{hex} the “vacuum” was assured with $c = 3.78 c_{\text{hex}}$, and the structure resulted in spacegroup D_{3d}^3 . The phonon dispersion is shown on the right panel of Fig. 2.

3 Experiment

By the use of a gas handling system and the control of the vapour pressure we have prepared well-defined amounts of Ar gas to condense in Gelsil glass with pore diameters of 75 \AA . The knowledge of the adsorption isotherm [5] allows to prepare a monolayer, two or three layers, and the capillary condensate.

It has been shown [5], that at low filling fractions the atoms form an amorphous adsorbate film smoothing out the rough pore walls due to an attractive adsorbate–substrate potential.

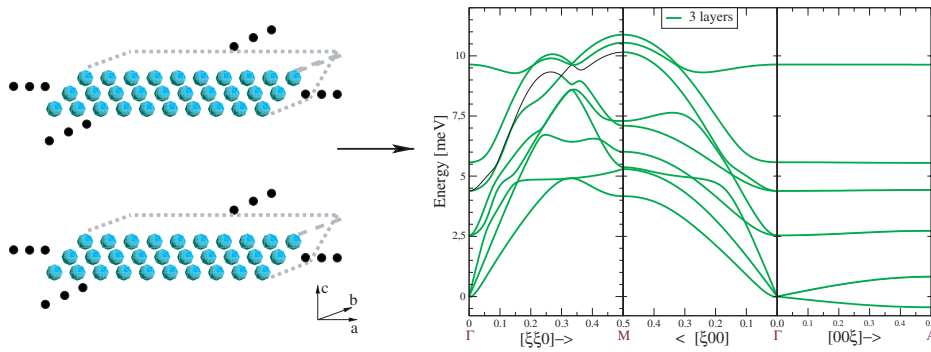


Fig. 2. Left: sketch of three layers of Ar atoms periodic in *a*- and *b*-direction and vacuum in *c*. Right: corresponding phonon dispersion in the main-symmetry directions.

The additionally adsorbed atoms can form more easily an ordered structure and reestablish a quasi-fcc pattern at complete fillings. Ar condensed in pores shows reflections as expected for an fcc solid, justifying the approximation by our model. Thus, the first few layers are expected to behave like a two-dimensional film and the completely filled pore similar to the bulk state.

The experiments were carried out on the time-of-flight spectrometer IN4 at the Institut Laue-Langevin, Grenoble, France. Inelastic data have been taken at $T = 5$ K with the incident neutron wavelength $\lambda = 2.24$ Å. Energy transfers up to 12 meV were accessible at the neutron energy-loss side. The data have been corrected for empty can and background scattering and normalised to a vanadium standard. The incoherent approximation was applied, and the DOS has been normalised to 1 mode in the energy range 1–12 meV.

4 Results and discussion

The upper panel of Fig. 3 shows the experimental DOS. The lower panel shows the theoretical DOS for bulk and the three-layer system of Ar. The energy axis of the calculated curves has been scaled by a factor of 0.75 to match the experimental one-phonon cut-off reported in Fig. 1. The frequencies of Ar monolayer weakly adsorbed on graphite (where the Ar–Ar interaction

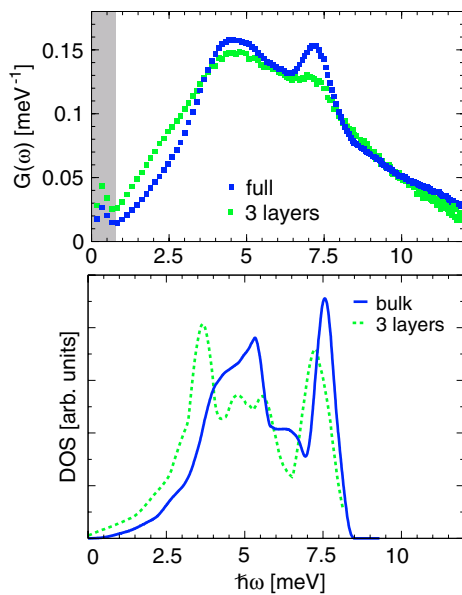


Fig. 3. Upper panel: experimental DOS for full filling and three layers. The shaded area shows the energy resolution. Lower panel: theoretical DOS for bulk and three layers of Ar, convoluted with a resolution of 0.5 meV (HWHM).

dominates) or calculated and measured for a monolayer are at about 3.5 and 6 meV, respectively, at the Brillouin-zone boundary [6,7]. That is similar to where the main dynamical features in our experimental and calculated data can be found indicating a similarly weak glass–adsorbent interaction. The overall two-peak structure is found in all four spectra; another similarity is the expected shift to lower frequencies. In addition to this general frequency shift to lower energies due to weak (or missing) bonds there is another effect: Whereas the phonon DOS $G(\omega)$ in a 3D system behaves like $G(\omega) \propto \omega^2$, the DOS of a 2D layer is $G(\omega) \propto \omega^1$ for small ω . This is a fingerprint of the reduced dimensionality, leading to an additional enhancement of 2D over 3D modes at small ω . Such an excess of the DOS of layered Ar over the bulk system at small energies can be seen in the theoretical results as well as in the experimental data in Fig. 3. Beyond the low-energy regime we can equally reproduce in the calculated spectra the general trends of the experimental intensity distribution. This is for example the overall reduction of intensity at $\hbar\omega > 3$ meV. However, differences between experiment and calculation are apparent. Even though we have smoothed the theoretical results with the experimental resolution function, the experimental data are much more washed out; this indicates an appreciable effect of defect broadening. If one imagines an additional broadening in the theoretical spectra, then the first peak in the bulk spectrum should have a shoulder on the high-energy side. In contrast, the experimental spectrum for full filling shows the enhancement on the low-energy side. This lets us conclude that a certain amount of bonds is weakened, consistent with the assumption of a defective structure. Besides idealised assumptions about the realistic systems differences could arise due to experimental conditions like energy resolution and, above 8 meV, multiple-scattering effects.

Except for the width, the peak at about 7.5 meV is very similar in theory and experiment. Thus, the general reproducibility of the features of the experimental data points out that their origin is to be found in the reduced dimensionality of the layered argon system.

5 Conclusion

The confinement of Ar in Gelsil glass influences its vibrational spectrum compared with the bulk system, e.g., an excess of modes at low energies $\hbar\omega < 3$ meV and a reduction of the spectral density at $\hbar\omega > 3$ meV has been experimentally established. While the overall features could be reproduced from ab-initio calculations of free Ar layers and bulk Ar, the detailed examination shows that the experimental full-pore system is not perfectly crystalline, but contains defects.

References

1. See the collection of articles in Eur. Phys. J. E **12** (Suppl.) (2003) 1–204 (electronic only)
2. X. Gonze et al., Comp. Mat. Sci. **25**, 478–492 (2002)
3. Y. Fujii et al., Phys. Rev. B **10**, 3647–3659 (1974)
4. T.M. Hakim, H.R. Glyde, Phys. Rev. B **41**, 1640–1644 (1990)
5. P. Huber, K. Knorr, Phys. Rev. B **60**, 12657–12665 (1999)
6. H. Taub et al., Phys. Rev. Lett **34**, 654–657 (1975)
7. H. Taub et al., Phys. Rev. B **16**, 4551–4567 (1977)